J Mater Sci: Mater Med (2010) 21:1163–1168
DOI 10.1007/s10856-009-3984-x

Kinetic studies of a composite carbon nanotube-hydrogel for tissue engineering by rheological methods

Fan Xie · Pierre Weiss · Olivier Chauvet ·
Jean Le Bideau · Jean François Tassin

Received: 8 October 2009 / Accepted: 23 December 2009 / Published online: 6 January 2010

Abstract Here we used rheological methods to study the gelation kinetics of silanized hydroxypropylmethylcellulose (HPMC-Si) hydrogel for tissue engineering. Firstly, the gelation time was determined from the independence of tan δ on frequency, and the Arrhenius law was applied to obtain the apparent activation energy of gelation, which was found to be about 109.0 kJ/mol. Secondly, the gelation process was monitored by measuring the sample storage modulus. The results showed that the gelation process could be well classified as a second-order reaction. In addition, a composite HPMC-Si/MWNTs hydrogel system for potential cartilage tissue engineering was investigated. The comparison of pure HPMC-Si hydrogel and composite HPMC-Si/MWNTs systems indicated that the addition of MWNTs could increase the mechanical strength of hydrogel without changing the gelation mechanism of the system.

1 Introduction

As alternative biomaterials used in tissue engineering, hydrogels have attracted much attention over the decades due to their good biocompatibility and high permeability for oxygen, nutrients, and other metabolites [1–3]. Cellulose and cellulose derivatives are the most abundant polymers in nature and have been used extensively to produce hydrogels for applications such as artificial implants and drug delivery. Hydroxypropylmethylcellulose (HPMC) is one of such cellulose derivative polymers.

Weiss et al. [4, 5] were the first to devise and study an injectable suspension for tissue engineering by mixing HPMC solution and biphasic calcium phosphate granules. These materials provided good biocompatibility and proper rheological properties for convenient injection but displayed a tendency to spread after implantation in vivo. For this reason, Weiss et al. [6, 7] developed biomaterials by grafting silane on HPMC, which forms a self-hardening silanized HPMC (HPMC-Si), without using any toxic chemical catalyst. The results showed that the hydrogel (HPMC-Si) provided excellent biocompatibility and bioactivity [8–11], which renders it a promising tissue engineering material.

Carbon nanotubes (CNTs) have been studied for many years for their potentially wide applications. One of the areas of research is the biomedical field [12]. Certain investigations have demonstrated that multi-walled carbon nanotubes (MWNTs) could provide structural reinforcement for tissue scaffolding of biomaterials and the mechanical strength of bio-composites could be greatly improved by incorporating and dispersing a small fraction of carbon nanotubes into biomaterials [13, 14]. However, contradictory results have also been reported showing that the ultimate strength of composite hydrogels declines as the percentage of CNTs increase [15]. More investigations into composite hydrogels are thus necessary.

In this study, we determined the apparent activation energy of gelation by investigating the gelation times of

F. Xie · P. Weiss (✉)
INSERM, U791, Laboratoire d'Ingénierie Ostéo-Articulaire
et Dentaire, Faculté de chirurgie dentaire, Université de Nantes,
44042 Nantes, France
e-mail: pweiss@sante.univ-nantes.fr

O. Chauvet · J. Le Bideau
Institut des Matériaux de Nantes, IMN, UMR 6502 CNRS
Université de Nantes, 44322 Nantes, France

J. F. Tassin
CNRS, UMR 6120, Laboratoire Polymères, Colloïdes,
Interfaces, Université du Maine, Avenue Olivier Messiaen,
72085 Le Mans, France

HPMC-Si hydrogels at different temperatures. The storage modulus was monitored in order to observe the gelation process. Reaction kinetics equations were also employed to determine the reaction order of the gelation process in HPMC-Si hydrogels. In addition, MWNT was incorporated into the pure HPMC-Si system and an appraisal was made of effects of the MWNT on the HPMC-Si hydrogels.

2 Materials and methods

2.1 Preparation of HPMC-Si and HPMC-Si/MWNTs hydrogels

The hydroxypropylmethylcellulose (HPMC) (Methocel® E4M, Colorcon-Kent-England) used in this study is a natural grade product and the weight average molecular weight is about 290,000 g/mol as determined by light scattering [7]. Both 3-glycidoxypropyltrimethoxysilane (GPTMS), which is the group to be grafted, and 4-(2-hydroxyethyl)-1-piperazineethanesulfonic acid (HEPES) were supplied by Aldrich (Germany). The multi-walled carbon nanotubes were prepared by the chemical vapour deposition (CVD) method. The outer diameters of MWNTs ranged from 10 to 30 nm, while the lengths were between 1 and 10 μm.

The HPMC was firstly silanized with GPTMS using the method described previously in details [7]. Following this, 6 g HPMC-Si were dissolved in 200 ml sodium hydroxide solution ([NaOH] = 0.2 M) at 25°C for 48 h, followed by dialysis against basic solution ([NaOH] = 0.09 M) for 16 h. The final pH value of the HPMC-Si basic solution was about 12.7. A buffer solution with a pH value of 3.7 was prepared by dissolving 6.2 g HEPES in an acid solution which was composed of 1.8 g NaCl and 60 ml HCl (0.1 M). All the solutions were sterilized by steam at 121°C for about 1 h for future use.

Two concentrations of MWNTs (0.01 and 0.03 wt%) were considered. The composite hydrogels were prepared by firstly dispersing the MWNTs in the buffer solution. Ultrasonication (XL2000 Misonix) for 60 min was performed to disperse the MWNTs. Next, one volume of HPMC-Si solution was mixed with a half volume of buffer/MWNTs blending solution, and the pH value of the final solution was about 7.4. Pure HPMC-Si hydrogel was also obtained when one volume of HPMC-Si solution was mixed with a half volume of pure buffer solution.

2.2 Rheological measurements

As the samples underwent a rapid gelation in our experiments, the mixing time of the HPMC-Si solution and buffer/MWNTs blending solution (or pure buffer solution) was limited to 3 min. After mixing solutions, samples were put into a rotational rheometer (RheoStress 300, Thermo-Haake Co., Germany) and the rheological properties of the samples were monitored in different modes under oscillatory shear with a selected titanium cone-plate geometry (60 mm diameter, 1° cone angle). A ring with oil was used to cover the free surface of the samples in order to prevent evaporation of solvent during measurements. The stress amplitude was set to 0.5 Pa, which lies in the linear viscoelastic region.

According to knowledge [16–18] derived from the percolation theory, at the gel point, the storage modulus, G', and the loss modulus, G'', obey the common power law, $G' \sim G'' \sim \omega^n$, over a range of frequencies. The ratio G''/G' at gelation time can be expressed as

$$\tan\delta = G''(\omega)/G'(\omega) = \tan(n\pi/2) \tag{1}$$

where n is the relaxation exponent. The phase angle between stress and strain, δ, is independent of frequency but proportional to the relaxation exponent

$$\delta = n\pi/2. \tag{2}$$

This implies that all the curves of tan δ versus time at different frequencies have a common intersection point which defines the gelation time [19, 20]. Due to rapid gelation, multi-wave mode [21] was used to monitor the samples. As the sweeping test time should be much smaller than the characteristic time of sample evolution, the frequency range was set from 1 to 30 rad/s.

2.3 Morphology characterization

Samples were further characterized by scanning electron microscopy (SEM). Briefly, the samples were frozen to rupture and then freeze-dried under vacuum overnight. A scanning electron microscope (Leo 1450 VP) was used to observe the morphology of the failure surfaces of the hydrogel samples at 10.0 kV.

2.4 Statistical analysis

Data in Table 2 were expressed as mean ± standard deviation (SD) for $n = 3$ and analyzed using a standard Student's *t*-test. Differences were considered significant when $P < 0.05$.

3 Results and discussion

3.1 Determination of gelation time

In pure hydrogel, the temporal variations of tan δ as a function of time during the gelation process at different

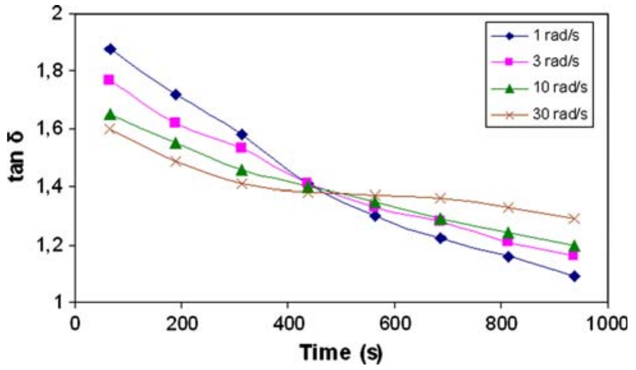

Fig. 1 Variations of tan δ of pure hydrogel as a function of time around the gel point in different frequencies at 25°C

Table 1 The critical gelation times of pure hydrogels at different temperatures

	20°C	25°C	30°C	35°C
t_g (s)	850	460	230	95

frequencies are shown in Fig. 1. The values of tan δ decreased with time at all frequencies, indicating that the samples were becoming more elastic as time increased. The gel point can be obtained easily from the intersection point where the value of tan δ was independent of frequency. The critical gelation times (t_g), where the gel points lie, at different temperatures are listed in Table 1. Apparent activation energy of the gelation processes can be obtained through an apparent Arrhenius law [19]. The kinetic equation can be expressed as

$$ln(t_g) = A + E_a/RT \tag{3}$$

where A is a constant, E_a is the apparent activation energy, and R is the gas constant. Figure 2 shows plots of gelation time versus $1/T$ in a semi-logarithmic scale and the apparent activation energy was found to be 109.0 kJ/mol.

The critical gelation times of composite hydrogels and the relaxation exponents at those points are shown in Table 2. It can be seen that the critical gelation times of composite HPMC-Si/MWNTs hydrogels show no significant difference compared to those of pure HPMC-Si hydrogels ($P > 0.05$), which indicates that the incorporation of MWNTs into pure hydrogels does not have a significant effect on the gelation process of the system. The relaxation exponents of composite hydrogels were also similar to those of pure hydrogels, demonstrating that the gel structures were hardly affected by MWNTs.

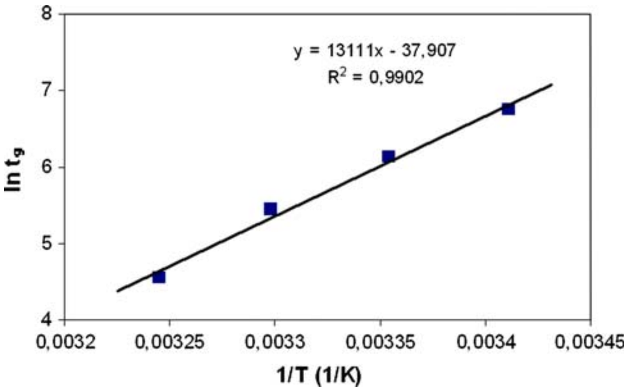

Fig. 2 Plots of gelation time (s) versus temperature given by Eq. 3

3.2 Kinetic process of gelation

According to the percolation theory [16], the elastic (viscous) part of the gel system G' (G'') can be expressed as $G' \sim \omega^2$ ($G'' \sim \omega$) below the gel point and $G' \sim const$ ($G'' \sim \omega$) above the gel point, which means that the storage modulus is more changeable than the loss modulus before and after the gel point. Typical storage modulus and loss modulus frequency curves are depicted in Fig. 3. It is obvious that, being dependent of frequency, the loss modulus of the system does not change with time, even after 5 days. At the same time, the storage modulus gradually increased with time and was consistently independent of frequency. These results indicate that the system gelates rapidly and then enters a long post-gel period. In addition, the values of the storage modulus were consistently much higher than those of the loss modulus, revealing the quasi-solid nature of the gel in the whole range of the investigated frequency [22].

As the storage modulus is independent of frequency, the time evolution of the storage modulus of the system is insensitive to the chosen frequencies. Figure 4 shows the evolutions of the storage modulus of different systems with time at a fixed angular frequency of 1 rad/s and at a temperature of 25°C. It can be seen that the storage modulus increased quickly at the beginning of the gelation and then slowed down over the processing time. The storage modulus of composite HPMC-Si/MWNTs hydrogels was slightly higher than that of pure HPMC-Si hydrogel,

Table 2 The critical gelation times and relaxation exponents of different hydrogels at 25°C

	Pure hydrogel	Composite hydrogel with MWNT (0.01 wt%)	Composite hydrogel with MWNT (0.03 wt%)
t_g (s)	460 ± 36	413 ± 55 ($P = 0.158$)*	456 ± 21 ($P = 0.404$)
n	0.586 ± 0.025	0.563 ± 0.027 ($P = 0.261$)	0.573 ± 0.004 ($P = 0.263$)

* P value is the result of comparing the value of composite hydrogel with the corresponding value of pure hydrogel by student's t-test

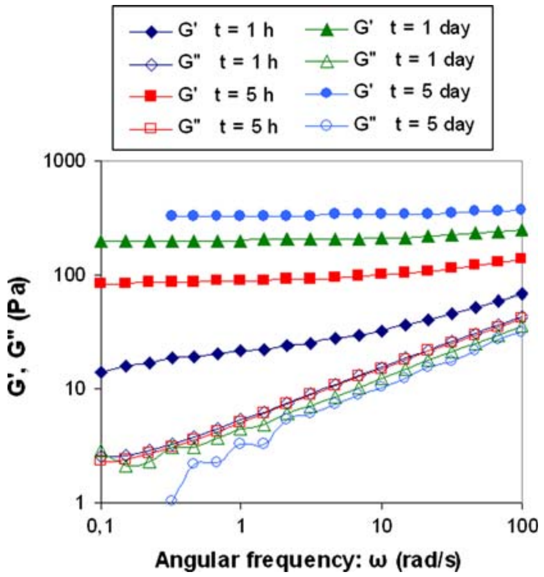

Fig. 3 Plots of storage modulus, G', and loss modulus, G'', as a function of frequency, ω, at 25°C in different times

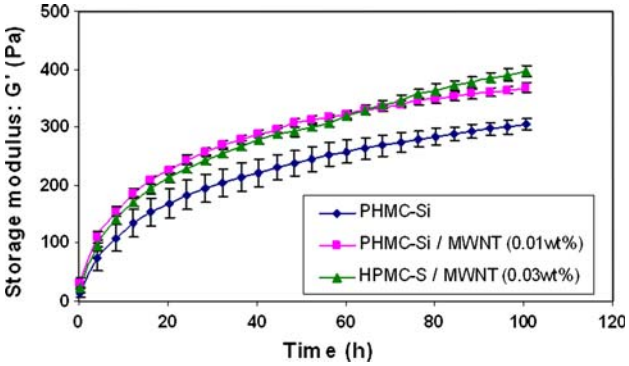

Fig. 4 Plots of storage modulus versus time for pure HPMC-Si hydrogel system and composite HPMC-Si/MWNTs hydrogel systems at 25°C

indicating that the addition of MWNTs to hydrogel increases the strength of the hydrogel.

A gel system is typified by its almost frequency-independent storage modulus (plateau modulus), which is associated with the number of cross-links in the network structure [23]. As a result, the reaction conversion $X(t)$ can be correlated with the change of storage modulus G' of the system as follows [24, 25]:

$$X(t) = [G'(t) - G'(0)]/[G'(\max) - G'(0)] \quad (4)$$

where $G'(t)$ is the value of the storage modulus at time t, and $G'(0)$ and $G'(max)$ are the values of the storage modulus at the start of the experiment and the maximum gelation time, respectively. Two kinds of simple reaction rate equations (the first and the second-order kinetics) were applied as follows:

$$-ln[1 - X(t)] = k_1 t \quad (5)$$

for the first-order reaction kinetics and

$$1/[1 - X(t)] = k_2 C_0 t + 1 \quad (6)$$

for the second-order reaction kinetics. Here, k_1 and k_2 are the reaction constants and C_0 is the initial concentration of reactive functional groups.

Figure 5 plots the conversion versus the reaction time based on the first-order reaction kinetics given by Eq. 5 and the second-order reaction kinetics given by Eq. 6 for different hydrogels. The data were vertically shifted by an arbitrary factor a in order to avoid overlapping. It is self evident that the reaction kinetics of a pure hydrogel system can be better described by a second-order reaction kinetics compared to a first-order reaction kinetics, which means that the gel process in our study is a second-order reaction. This result is in accordance with the reports of the curing reactions [24].

The conversion of composite HPMC-Si/MWNTs hydrogels versus reaction time based on the first and second-order reaction kinetics are also shown in Fig. 5. Obviously, there is little difference between the curve of pure hydrogel and those of composite hydrogels. This indicates that the incorporation of MWNTs has no effect on the mechanism of gelation of the system.

As the multi-walled carbon nanotubes used in the present study have not been functionalized and are thus

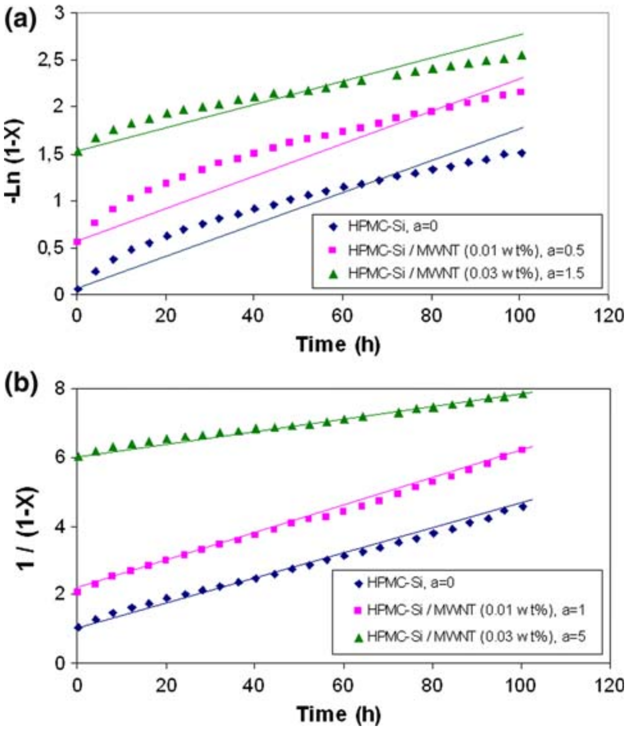

Fig. 5 Plots of conversion versus reaction time based on **a** the first-order reaction kinetics given by Eq. 5 and **b** the second-order reaction kinetics given by Eq. 6 for different hydrogels

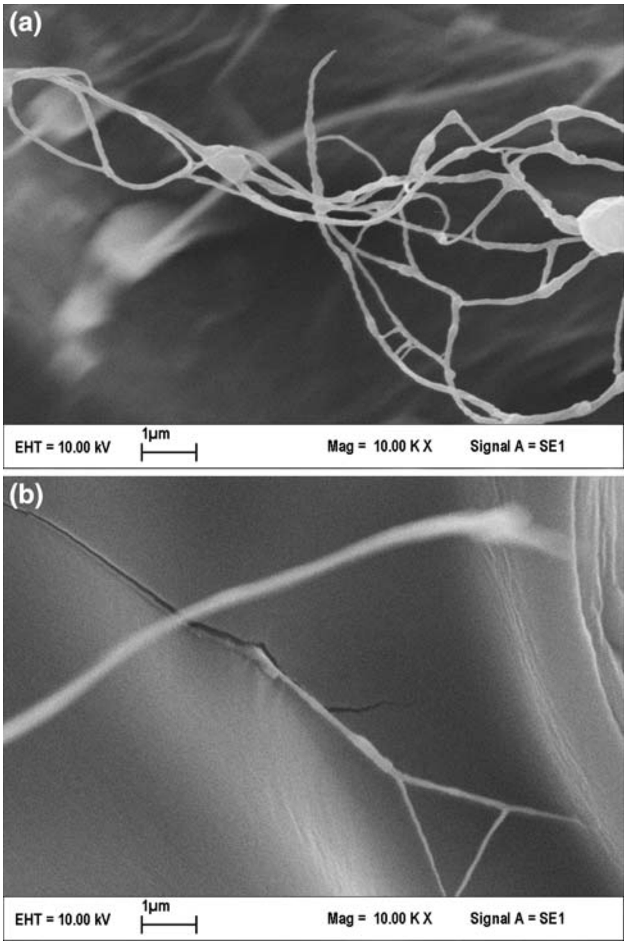

Fig. 6 SEM images of the morphologies of composite HPMC-Si/MWNTs system

hydrophobic, it was difficult to disperse the MWNTs in aqueous solutions. Although strong ultrasonication was used to disperse the MWNTs in the buffer solutions, carbon nanotubes had no difficulty in aggregating. As shown in Fig. 6, both isolated and aggregated carbon nanotubes could be observed by SEM in the gel. This suggests that the dispersion of carbon nanotubes still needs to be improved, although the macroscopically homogeneous appearance of the composite hydrogels can be obtained. It is worth pointing out that non-functionalized carbon nanotubes hardly form a tight connection with the hydrogel matrix since no chemical reaction occurs on their surface. This should prompt a limited improvement in the strength of composite hydrogels. In future studies, functionalized carbon nanotubes will be used to reinforce the hydrogels.

4 Conclusion

In the present study, the gelation kinetics of HPMC-Si hydrogel was investigated by rheological methods. The gelation times were measured at different temperatures and the apparent activation energy of gelation was found to be 109.0 kJ/mol. A good fit of the conversion curve to the second-order reaction kinetic line suggests that the gelation process in this study is second-order. In addition, the incorporation of MWNTs into the hydrogels increases the strength of the hydrogel system without affecting the mechanism of gelation.

Acknowledgment This research was supported by the regional program BIOREGOS (Pays de la Loire, France).

References

1. Suh JKF, Matthew HWT. Application of chitosan-based polysaccharide biomaterials in cartilage tissue engineering: a review. Biomaterials. 2000;21:2589–98.
2. Nguyen KT, West JL. Photopolymerizable hydrogels for tissue engineering applications. Biomaterials. 2002;23:4307–14.
3. Brandl F, Sommer F, Goepferich A. Rational design of hydrogels for tissue engineering: impact of physical factors on cell behavior. Biomaterials. 2007;28:134–46.
4. Weiss P, Gauthier O, Bouler JM, Grimandi G, Daculsi G. Injectable bone substitute using a hydrophilic polymer. Bone. 1999;25(2 Suppl.):67S–70S.
5. Schmitt M, Weiss P, Bourges X, Valle GA, Daculsi G. Crystallization at the polymer/calcium-phosphate interface in a sterilized injectable bone substitute IBS. Biomaterials. 2002;23:2789–94.
6. Turczyn R, Weiss P, Lapkowski M, Daculsi G. In situ self hardening bioactive composite for bone and dental surgery. J Biomater Sci Polym Ed. 2000;2:217–23.
7. Bourges X, Weiss P, Daculsi G, Legeay G. Synthesis and general properties of silated-hydroxypropyl methylcellulose in prospect of biomedical use. Adv Colloid Interface Sci. 2002;99:215–28.
8. Vinatier C, Magne D, Weiss P, Trojani C, Rochet N, Carle GF, et al. A silanized hydroxypropyl methylcellulose hydrogel for the three-dimensional culture of chondrocytes. Biomaterials. 2005;26:6643–51.
9. Merceron C, Vinatier C, Clouet J, Jouault SC, Weiss P, Guicheux J. Adipose-derived mesenchymal stem cells and biomaterials for cartilage tissue engineering. Joint Bone Spine. 2008;75:672–4.
10. Trojani C, Weiss P, Michiels JF, Vinatier C, Guicheux J, et al. Three-dimensional culture and differentiation of human osteogenic cells in an injectable hydroxypropylmethylcellulose hydrogel. Biomaterials. 2005;26:5509–17.
11. Trojani C, Boukhechba F, Scimeca JC, Vandenbos F, Michiels JF, et al. Ectopic bone formation using an injectable biphasic calcium phosphate/Si-HPMC hydrogel composite loaded with undifferentiated bone marrow stromal cells. Biomaterials. 2006;27:3256–64.
12. Harrison BS, Atala A. Carbon nanotube applications for tissue engineering. Biomaterials. 2007;28:344–53.
13. Wang SF, Shen L, Zhang WD, Tong YJ. Preparation and mechanical properties of chitosan/carbon nanotubes composites. Biomacromolecules. 2005;6:3067–72.
14. Bhattacharyya S, Guillot S, Dabboue H, Tranchant JF, Salvetat JP. Carbon nanotubes as structural nanofibers for hyaluronic acid hydrogel scaffolds. Biomacromolecules. 2008;9:505–9.
15. Wang Z, Chen Y. Supramolecular hydrogels hybridized with single-walled carbon nanotubes. Macromolecules. 2007;40: 3402–7.v

16. Axelos MAV, Kolb M. Crosslinked biopolymers: experimental evidence for scalar percolation theory. Phys Rev Lett. 1990;64:1457–60.
17. Scanlan JC, Winter HH. Composition dependence of the viscoelasticity of end-linked poly(dimethylsiloxane) at the gel point. Macromolecules. 1991;24:47–54.
18. Richtering HW, Gagnon KD, Lenz RW, Fuller RC, Winter HH. Physical gelation of a bacterial thermoplastic elastomer. Macromolecules. 1992;25:2429–33.
19. Ponton A, Warlus S, Griesmar P. Rheological study of the sol-gel transition in silica alkoxides. J Colloid Interface Sci. 2002;249:209–16.
20. Ponton A, Doeuff SB, Sanchez C. Physico-chemical control of sol-gel transition of titanium alkoxide-based materials studied by rheology. J Non-cryst Solids. 2005;351:45–53.
21. Kavanagh GM, Murphy SBR. Rheological characterisation of polymer gels. Prog Polym Sci. 1998;23:533–62.
22. Misawa Y, Koumura N, Matsumoto H, Tamaoki N, Yoshida M. Hydrogels based on surfactant-free ionene polymers with *N*,*N*′-(*p*-phenylene)dibenzamide linkages. Macromolecules. 2008;41:8841–6.
23. Böhm N, Kulicke WM. Rheological studies of barley (1 → 3)(1 → 4)-*β*-glucan in concentrated solution: mechanistic and kinetic investigation of the gel formation. Carbohydr Res. 1999;315:302–11.
24. Madbouly SA, Otaigbe JU. Kinetic analysis of fractal gel formation in waterborne polyurethane dispersions undergoing high deformation flows. Macromolecules. 2006;39:4144–51.
25. Zlatanic A, Dunjic B, Djonlagic J. Rheological study of the copolymerization reaction of acrylate-terminated unsaturated copolyesters with styrene. Macromol Chem Phys. 1999;200:2048–58.